Bull. Chem. Soc. Jpn., 70, 1583—1592 (1997)

Formation of Di- and Tricarbonylruthenium(O) Species from $[RuH_2(CO)(PPh_3)_3]$ via Decarbonylation of Methyl Benzoates: X-Ray Crystal Structures of $[Ru(CO)_2(PPh_3)_3]$ and $[Ru(O_2)(CO)_2(PPh_3)_2]$

Katsuma Hiraki,* Shu-ichi Kira, and Hiroyuki Kawano†

Department of Applied Chemistry, Faculty of Engineering, Nagasaki University, Bunkyo-machi, Nagasaki 852

†Graduate School of Marine Science and Engineering, Nagasaki University, Bunkyo-machi, Nagasaki 852

(Received December 6, 1996)

Dihydridoruthenium(II) complex $[RuH_2(CO)(PPh_3)_3]$ (**1**) reacts with methyl benzoate in the presence of an olefin at 110 °C to afford some dicarbonylruthenium(O) species $[Ru(CO)_2(PPh_3)_3]$ (**2**) and "$Ru(CO)_2(PPh_3)_2L$" (L = the olefin or the ester). A tricarbonylruthenium(O) complex $[Ru(CO)_3(PPh_3)_2]$ (**3**) is formed at higher reaction temperature. The experiment using ^{13}C-enriched methyl benzoate reveals that the second and the third carbonyl ligands are mainly derived by subtraction of the carbonyl group from the ester. When the reaction is carried out in the presence of triethoxyvinylsilane, a part of the second and the third carbonyl groups is derived from the ethoxy group of the silane, because **1** reacts with the silane at 110 °C in the absence of the ester to afford **2** and **3**. The formation ratio of **2** and **3** is affected by the type of olefins used; selective formation of **2** and **3** is achieved when triethoxyvinylsilane is used, whereas allylbenzene or cyclooctene affords merely a mixture of the di- and tricarbonyl species. The reaction mixture containing **2** and "$Ru(CO)_2(PPh_3)_2L$" is exposed to air to give a peroxo complex $[Ru(\eta^2\text{-}O_2)(CO)_2(PPh_3)_2]$ (**4**) smoothly. The molecular structures of **2** and **4** are determined by the single crystal X-ray diffraction method. The complex **2** has a distorted trigonal bipyramidal coordination geometry with two equatorial CO ligands, whereas the complex **4** has a distorted octahedral structure.

Ruthenium complex-catalyzed carbon–carbon bond formations are current topics in organometallic chemistry.[1—5] Recently, Murai and co-workers[6] found an epoch-making reaction in this area: a novel coupling reaction between terminal olefins and aromatic ketones was catalyzed by $[RuH_2(CO)(PPh_3)_3]$ (**1**) or $[Ru(CO)_2(PPh_3)_3]$ (**2**) to give the corresponding *o*-substituted derivatives. They proposed a plausible mechanism, where a zerovalent ruthenium species evolved in the catalytic cycle and underwent oxidative addition of the C–H bond of the ketone to give an orthometallated hydridoruthenium(II) species as an intermediate. Later researchers have reported other catalytic carbon–carbon bond-forming reactions via a similar C–H bond activation: ruthenium complex-catalyzed coupling reactions,[7,8] an acylation of imidazoles,[9] and a rhodium complex-catalyzed coupling reaction.[10]

We have worked on the insertion of vinyl compounds[11] and allylic compounds[12,13] into the Ru–H bond of a hydridoruthenium(II) complex $[RuClH(CO)(PPh_3)_3]$. In the course of our investigations on the chemistry of hydridoruthenium(II) complexes, we have been studying the reactions of **1** in the presence of unsaturated organic compounds. In the reaction of terminal olefins and some benzoic acid esters with a catalytic amount of **1**, we have found that only little amounts of *o*-substituted esters are produced in spite of Murai's coupling reaction conditions. Furthermore, the catalyst precursor **1** is converted into di- and tricarbonylruthenium(O) species such as $[Ru(CO)_2(PPh_3)_3]$ and $[Ru(CO)_3(PPh_3)_2]$ (**3**) in the reaction mixture. Here we report details of the formation of the di- and tricarbonylruthenium(O) species via subtraction of the carbonyl group of the benzoates. The molecular structures of **2** and $[Ru(\eta^2\text{-}O_2)(CO)_2(PPh_3)_2]$ (**4**) are also discussed.

Results and Discussion

Isolation and Molecular Structure of $[Ru(CO)_2(PPh_3)_3]$. A dihydridoruthenium(II) complex $[RuH_2(CO)(PPh_3)_3]$ (**1**) reacted with methyl benzoate in the presence of triethoxyvinylsilane in octane at 110 °C to give a zerovalent ruthenium species $[Ru(CO)_2(PPh_3)_3]$ (**2**), which had been prepared previously from $[RuH(CO)_2(PPh_3)_3]BF_4$ and sodium methoxide by Roper et al.[14] Our method provides a convenient short route to **2**, which is very useful as a catalyst precursor[6] and a starting complex for various ruthenium complexes[14] (Scheme 1).

The single crystal X-ray analysis of **2** revealed a unique crystal structure as shown in Fig. 1. Selected bond lengths and angles are summarized in Table 1. The single crystal of **2** contains two independent molecules in its asymmetric unit. These two molecules are essentially similar but have somewhat different conformations from each other; in other words, two sets of three P–C bonds of the apical PPh_3 ligands

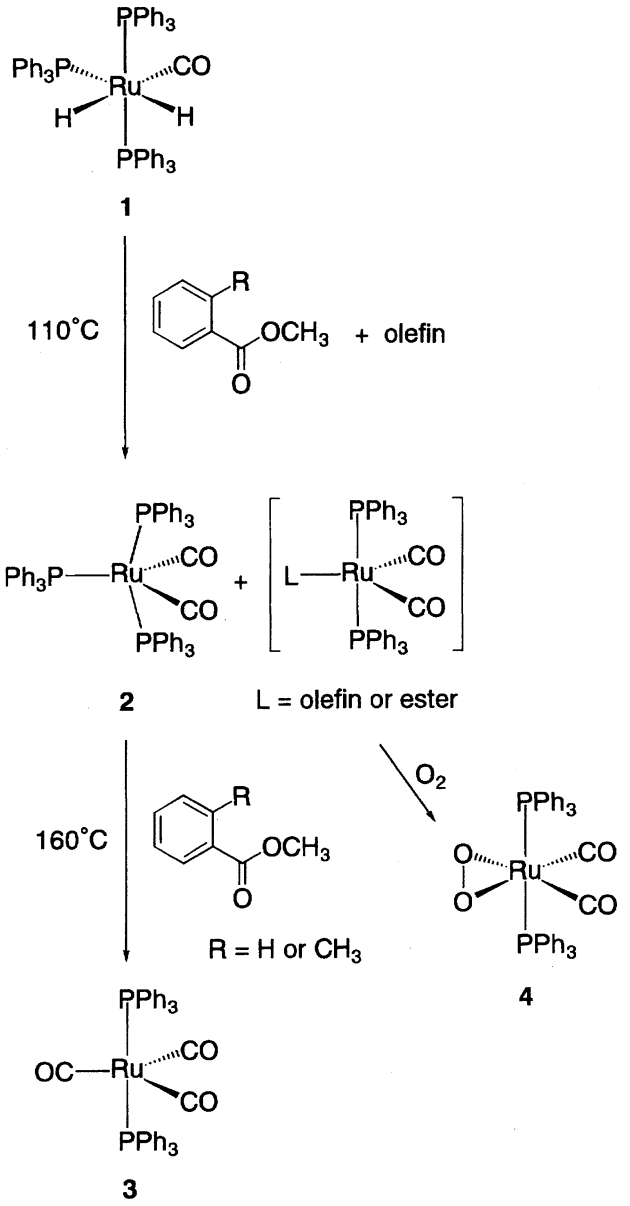

Scheme 1.

were aligned in an eclipsed manner in molecule I, whereas they were oriented slightly staggered in molecule II.

Two characteristic features are found in the molecular structure of **2**. The first feature is a strongly distorted trigonal bipyramidal arrangement around the ruthenium center. Six atoms of the Ru, the equatorial P (P_{eq}), and the two CO ligands in each molecule are situated actually upon an equatorial plane with mean deviations of 0.0692 and 0.0472 Å for molecules I and II, respectively. Bond angles among the two apical P (P_a) and the Ru center (153.35(9)° and 158.17(9)° for I and II, respectively) are fairly smaller than 180°. This compression of the P_a–Ru–P_a angles is probably due to steric repulsion between the equatorial and the apical PPh_3 ligands. On the other hand, C–Ru–C angles (144.5(5)° and 133.7(4)° for I and II, respectively) are much larger than the 120° expected for trigonal bipyramidal coordination geometry in order to avoid steric hindrance with the two apical PPh_3 ligands. The dilatation of these C–Ru–C angles can be related to the compression of the P_a–Ru–P_a angles. Therefore, the arrangement of the PPh_3 and CO ligands of **2** seemingly lies in the middle of Berry's pseudo-rotation[15] from a trigonal bipyramidal geometry to a square pyramidal one.

The second feature is that Ru–P_{eq} bond lengths (2.399(2) and 2.424(2) Å for I and II, respectively) are longer than those between the Ru and P_a atoms. The Ru–P_{eq} bond lengths fall within the reported values for Ru–PPh_3 bonds, but are among the longest ones reported.[16] This is consistent with the fact that the equatorial PPh_3 of **2** can be dissociated easily and replaced by another ligand in solution. Such ligand exchange reactions of **2** were reported in the literature.[14]

Ogasawara et al. reported the preparation and molecular structures of a related four-coordinate $[Ru(CO)_2(PBu^t{}_2Me)_2]$[17] and a five-coordinate $[Ru(CO)_2(PPr^i{}_2Me)_3]$.[18] The structure of the four-coordinate 16-electron species is viewed as a fragment of a distorted trigonal bipyramid, where one of the equatorial sites remains unoccupied and the other two are occupied by CO ligands. A comparison of our five-coordinate structure with that of $[Ru(CO)_2(PBu^t{}_2Me)_2]$ shows that the coordination of the equatorial phosphine brings about only a slight structural change of the other four ligands. Firstly, the P_a–Ru–P_a angles of **2** are bent more strongly than that of $[Ru(CO)_2(PBu^t{}_2Me)_2]$ (165.56(8)°) because of the steric repulsion between the equatorial and apical PPh_3 ligands. Secondly, the Ru–C–O bonds of the four-coordinate complex (168.2(8)° and 168.7(7)°) are bent significantly, whereas those of **2** (173.8(8)°—175.2(8)°) are less bent. As for the five-coordinate complex, the unit cell of $[Ru(CO)_2(PPr^i{}_2Me)_3]$ contained two independent molecules just like as that of **2** does. One of the two (the C–Ru–C angle was 146.68(18)°) resembled both conformers of **2** with a square pyramidal-like structure. But the other, interestingly, was a trigonal bipyramid with angles between the ligands deviating from the ideal ones by less than 8°.

Roper et al.[14] reported previously that **2** was ascribed to a trigonal bipyramidal structure with the two CO ligands located on two apical sites on the basis of a single strong absorption at 1905 cm^{-1} in its IR spectrum. In our IR spectrum of **2** (KBr), however, a weak absorption is found at 1850 cm^{-1} in addition to the strong absorption at 1905 cm^{-1}. A similar IR absorption at 1856 cm^{-1} was observed in C_6D_6.[18] The weak band at the lower wavenumber implies the existence of the isomer where the two CO ligands are laid equatorial, and it is consistent with the X-ray molecular structure results in the solid state.

Formation of Di- and Tricarbonylruthenium(O) Complexes. When the reaction of **1** with methyl *o*-toluate and triethoxyvinylsilane was carried out in toluene at 110 °C for 3 h, all the products remained dissolved in the reaction mixture. The $^{31}P\{^1H\}$ NMR spectrum of the reaction mixture showed two major singlets at $\delta = -6.3$ and 48.7, and five weak singlets in the region of $\delta = 42.0$—56.3. The major singlet at $\delta = 48.7$ is ascribed to **2**, whereas the other at $\delta = -6.3$ is a signal of free PPh_3. The ^{31}P-signal of **2** was

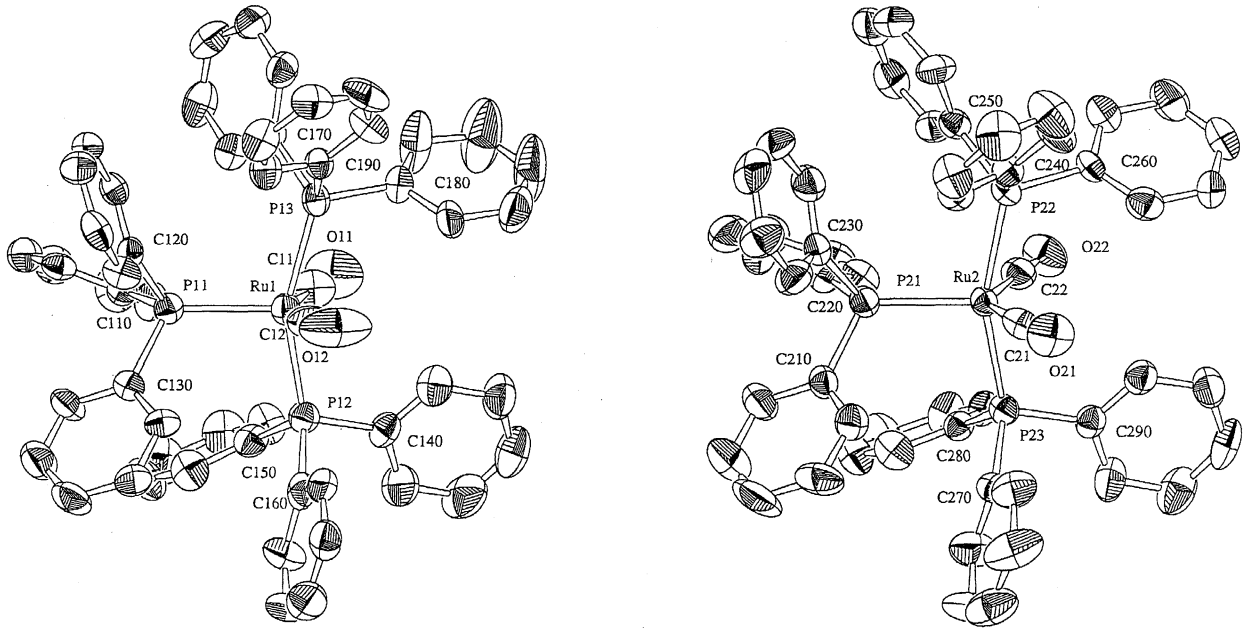

Fig. 1. Perspective views of the complex **2** including the atom-numbering scheme. Hydrogen atoms are omitted for clarity.

observed to be a singlet at any temperature between 30 and −80 °C as Gaffney and Ibers[19] originally detected the singlet at −48 °C. The fact that only one singlet can be observed, as opposed to two sets of A_2X signals expected for the crystal structure, implies the following fluxionalities of **2** in solution. One is the quick exchange among the apical and equatorial PPh_3 ligands in one molecule. The other is the rapid isomerization between the two forms of **2** found in the crystal. One of the small singlets (at $\delta = 54.8$) can be assigned to a tricarbonylruthenium(O) species $[Ru(CO)_3(PPh_3)_2]$ (**3**). After the reaction mixture was treated at 160 °C for a further 12 h, the $^{31}P\{^1H\}$ NMR spectrum exhibited only two singlets at $\delta = -6.3$ (PPh_3) and $\delta = 54.8$ (**3**) with an intensity ratio of 1 : 2. The complex **3** was isolated in good yield from the reaction mixture treated at 160 °C, and fully characterized by elementary analysis and spectroscopic analysis.[20]

The major singlet of **2** and the other four small singlets disappeared completely by heating at 160 °C. Since the four small singlets were all converted into that of the tricarbonyl species **3**, we expect these minor species may be attributed to some dicarbonyl species formulated as "$Ru(CO)_2(PPh_3)_2L$" (L = triethoxyvinylsilane or methyl *o*-toluate), and their related ruthenium(O) species. Coordination of olefins to dicarbonylruthenium(O) species has been well reported; for example, an ethylene complex $[Ru(C_2H_4)(CO)_2(PPh_3)_2]$ is obtained smoothly from **2** and ethylene in solution.[14] Recently, Mawby et al.[21] have reported that $[RuH_2(CO)_2(PMe_2Ph)L']$ (L′ = PMe_2Ph or $P(OMe)_3$) reacts with olefins RHC=CHR (R = H, CO_2Me, or CN) to afford the corresponding (olefin)-ruthenium(O) species, $[Ru(CO)_2(RHC{=}CHR)(PMe_2Ph)L']$.

The formation of **2** and **3** was examined in the presence of some olefins (Table 2). When terminal olefins such as triethoxyvinylsilane and allylbenzene were employed, the starting

Table 1. Selected Bond Lengths (Å) and Angles (deg) for **2**

Molecule I		Molecule II	
Bond length			
Ru(1)–P(11)	2.399(2)	Ru(2)–P(21)	2.424(2)
Ru(1)–P(12)	2.372(3)	Ru(2)–P(22)	2.347(3)
Ru(1)–P(13)	2.340(3)	Ru(2)–P(23)	2.374(3)
Ru(1)–C(11)	1.897(10)	Ru(2)–C(21)	1.862(9)
Ru(1)–C(12)	1.840(10)	Ru(2)–C(22)	1.865(9)
O(11)–C(11)	1.19(1)	O(21)–C(21)	1.186(9)
O(12)–C(12)	1.17(1)	O(22)–C(22)	1.182(9)
Bond angle			
P(11)–Ru(1)–P(12)	100.76(9)	P(21)–Ru(2)–P(22)	101.27(8)
P(11)–Ru(1)–P(13)	104.35(9)	P(21)–Ru(2)–P(23)	99.69(8)
P(11)–Ru(1)–C(11)	109.8(3)	P(21)–Ru(2)–C(21)	115.5(3)
P(11)–Ru(1)–C(12)	105.6(4)	P(21)–Ru(2)–C(22)	110.8(3)
P(12)–Ru(1)–P(13)	153.35(9)	P(22)–Ru(2)–P(23)	158.17(9)
P(12)–Ru(1)–C(11)	81.3(3)	P(22)–Ru(2)–C(21)	84.6(3)
P(12)–Ru(1)–C(12)	95.7(3)	P(22)–Ru(2)–C(22)	83.7(3)
P(13)–Ru(1)–C(11)	81.9(3)	P(23)–Ru(2)–C(21)	91.9(3)
P(13)–Ru(1)–C(12)	86.1(3)	P(23)–Ru(2)–C(22)	83.3(3)
C(11)–Ru(1)–C(12)	144.5(5)	C(21)–Ru(2)–C(22)	133.7(4)
Ru(1)–C(11)–O(11)	174(1)	Ru(2)–C(21)–O(21)	173.9(8)
Ru(1)–C(12)–O(12)	173(1)	Ru(2)–C(22)–O(22)	175.2(8)

1 was mostly consumed within 6 h. In contrast, both the consumption of **1** and the formation of **2** and **3** were very slow in the absence of olefin. Cyclooctene, an inner olefin, only slightly accelerated the reaction. These results support the assertion that there exists transfer hydrogenation of the olefin prior to the formation of the di- and tricarbonyl species. Without olefins, only the slow reductive elimination of dihydrogen was allowed, to bring about small amounts of Ru(O) intermediates. Such a slow reaction should be promoted by

Table 2. Effect of Olefins on the Reaction of **1** with Methyl Benzoate[a)]

Entry	Olefin	**1**/ester/olefin mmol	Time h	Conversion[b)] %	Yield[b)]/% **2**	**3**
1	None	0.02/0.14/—	3	8	Trace	2
2	None	0.02/0.14/—	6	13	2	5
3	None	0.02/0.14/—	24	27	Trace	7
4	Triethoxyvinylsilane	0.03/0.16/0.13	3	>99	67	18
5	Triethoxyvinylsilane	0.03/0.16/0.13	6	>99	60	24
6	Allylbenzene	0.02/0.13/0.13	3	84	24	58
7	Allylbenzene	0.02/0.13/0.13	6	96	23	70
8	Allylbenzene	0.02/0.13/0.13	24	>99	33	63
9	Cyclooctene	0.03/0.14/0.15	3	13	Trace	5
10	Cyclooctene	0.03/0.14/0.15	6	22	2	11
11	Cyclooctene	0.03/0.14/0.15	24	52	11	31

a) All reaction were carried out at 110 °C in toluene-d_8 (0.6 cm^3) in a sealed NMR tube. b) Determined by $^{31}P\{^1H\}$ NMR spectroscopy.

heat or light.

It is noteworthy that the type of the olefins affects the relative yields of **2** and **3**. When triethoxyvinylsilane was used for the reaction, the dicarbonyl species **2** was produced mainly and was slowly converted into the tricarbonyl species **3** at 110 °C. In the presence of allylbenzene or cyclooctene, in contrast, two or three times as much **3** was produced as **2**. As stated above, the olefin tends to coordinate to the intermediary dicarbonyl species in competition with the ester. Therefore, the coordination ability of these olefins explains such differences in the relative yields. Triethoxyvinylsilane, a terminal olefin, coordinates to the "$Ru(CO)_2(PPh_3)_2$" moiety to inhibit the subtraction of the third carbonyl group from the ester. On the other hand, cyclooctene hardly coordinates to the dicarbonyl species for steric reasons, and that allows the dicarbonyl species to react with the ester, forming the tricarbonyl species **3**. The high conversion achieved in the presence of allybenzene is due to the high reactivity of terminal olefin. However, allylbenzene, which played a role as a terminal olefin initially in the reaction, was completely isomerized into 1-phenylpropene within 3 h. Then it acts as an inner olefin after the isomerization. The catalytic isomerization into the inner olefin accounts for the relatively high yields of **3** given by allybenzene.

Formation and Molecular Structure of $[Ru(O_2)(CO)_2(PPh_3)_2]$ (4). When the reaction solution that contained mainly the dicarbonylruthenium(O) species was exposed to air, orange crystals of $[Ru(O_2)(CO)_2(PPh_3)_2]$ (**4**) were precipitated smoothly. The complex **4** had previously been prepared and characterized by Roper et al.[14] Our IR data of **4** were consistent with those reported.

The results of FAB-MS analysis of **4** gave a proof to the coordination of dioxygen. Peaks centered at *m/z* 713 $[M-1]^+$ showed a characteristic distribution for a monoruthenium species according to the isotopes of ruthenium. Peaks of some oxoruthenium species and $Ru(CO)_m(PPh_3)_n$ ($m+n\leq 4$) were also found with a similar isotopic pattern, in addition to the peak of $Ph_3P{=}O$ in the spectra. The oxoruthenium species and $PPh_3{=}O$ must be generated during the fragmentation process.

The molecular structure of **4** was determined as shown in Fig. 2. Selected bond lengths and angles are summarized in Table 3. Two PPh_3 ligands are situated trans to each other; P(1)–Ru–P(2) angle is 173.1(1)° and not so far removed from 180°. The O(1)–O(2) distance is 1.468(10) Å, longer than that of free dioxygen molecule (1.27 Å), close to an average value for the reported dianionic η^2-O_2 ligands (1.460(26) Å),[16] and especially the same as that of $[Ru(\eta^2\text{-}O_2)(CO)_2(PBu^t{}_2Me)_2]$ (1.472(10) Å)[17b] within error. The O(1)–Ru–O(2) angle (41.2(3)°) is considerably small for an octahedral six-coordinate structure. Such a distorted octahedral geometry was also found in isoelectronic rhodium(III) and iridium(III) complexes, $[Rh(\eta^2\text{-}O_2)(dppe)_2]PF_6$,[22] $[Ir(\eta^2\text{-}O_2)(dppe)_2]PF_6$,[22] and $[RhCl(\eta^2\text{-}O_2)(PPh_3)_3]$.[23]

Formation Mechanism of the Di- and Tricarbonylruthenium(O) Species. Plausible routes from the starting

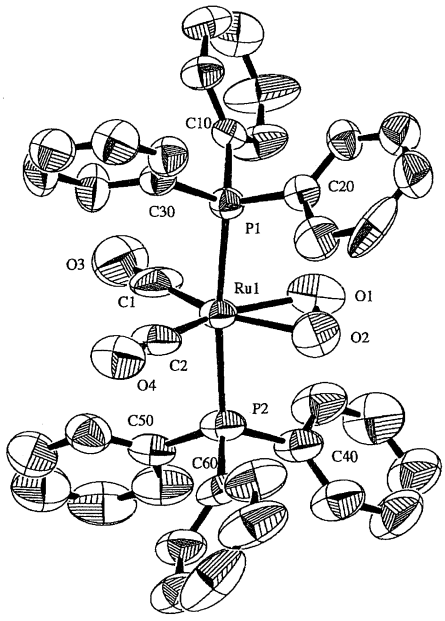

Fig. 2. A perspective view of the complex **4** including the atom-numbering scheme. Hydrogen atoms are omitted for clarity.

Table 3. Selected Bond Lengths (Å) and Angles (deg) for **4**

Bond length			
Ru(1)–P(1)	2.375(2)	Ru(1)–C(1)	1.87(1)
Ru(1)–P(2)	2.378(3)	Ru(1)–C(2)	1.828(10)
Ru(1)–O(1)	2.092(8)	O(3)–C(1)	1.15(1)
Ru(1)–O(2)	2.079(8)	O(4)–C(2)	1.160(10)
O(1)–O(2)	1.468(9)		
Bond angle			
P(1)–Ru(1)–P(2)	173.1(1)	O(1)–Ru(1)–O(2)	41.2(3)
P(1)–Ru(1)–O(1)	83.9(2)	O(1)–Ru(1)–C(1)	111.1(5)
P(1)–Ru(1)–O(2)	89.7(2)	O(1)–Ru(1)–C(2)	153.5(4)
P(1)–Ru(1)–C(1)	90.9(3)	O(2)–Ru(1)–C(1)	152.0(5)
P(1)–Ru(1)–C(2)	92.5(3)	O(2)–Ru(1)–C(2)	112.8(4)
P(2)–Ru(1)–O(1)	91.1(2)	C(1)–Ru(1)–C(2)	95.2(5)
P(2)–Ru(1)–O(2)	83.4(2)	Ru(1)–C(1)–O(3)	176(1)
P(2)–Ru(1)–C(1)	95.3(3)	Ru(1)–C(2)–O(4)	177(1)
P(2)–Ru(1)–C(2)	90.0(3)		

1 to the di- and tricarbonyl species **2** and **3** are depicted in Scheme 2.

The first step is formation of ruthenium(O) intermediates via hydrogenation of an olefin. It is widely recognized that a ruthenium(O) species can be formed by the removal of the hydrides of **1** by an olefin.[4–6,22] In fact, the ^{1}H NMR and GC-MS analyses revealed the presence of triethoxyethylsilane in our reaction mixture. This is an unambiguous proof of the initial transfer hydrogenation of triethoxyvinylsilane with **1**. The ruthenium(O) species thus formed should be a series of "Ru(CO)(PPh_3)$_3$L" (L = olefin or ester) or an orthometallated Ru(II) complex [Ru($C_6H_4PPh_2$)H(CO)(PPh_3)$_2$][24] in solution, because the monocarbonyl four-coordinate 16-electron species "Ru(CO)(PPh_3)$_3$" must be unstable without the fifth ligand.

Since it was supposed that the second and the third carbonyl ligands of **2**—**4** were derived from carbonyl group of the ester, ^{13}C-enriched methyl benzoate ($C_6H_5{}^{13}COOCH_3$) was used for the reaction with **1** and triethoxyvinylsilane. After the reaction at 110 °C for 3 h, the ^{13}C{^{1}H} NMR spectrum of the reaction mixture showed two enhanced signals at δ = 221.5 (quartet) and at δ = 208.6 (triplet), which were attributed to [Ru(^{13}CO)(^{12}CO)(PPh_3)$_3$] and [Ru(^{13}CO)$_2$(^{12}CO)(PPh_3)$_2$], respectively. Additional treatment at 160 °C for 3 h converted the dicarbonyl species into the tricarbonyl species. The ^{13}C{^{1}H} NMR spectrum showed the enlarged triplet of the ^{13}CO ligand at δ = 208.6. No other signal except for the ^{13}C-enriched ester was enhanced by ^{13}C throughout the experiment. These data indicate unequivocally that the second and third carbonyl ligands in **2**—**4** are derived from the carbonyl group of the ester. Consistently with the ^{13}C{^{1}H} NMR results, a large signal of the dicarbonyl **2** and a small signal of the tricarbonyl **3** were observed in the ^{31}P{^{1}H} NMR spectrum after 3 h at 110 °C. The former signal disappeared and the latter grew larger after the treatment at 160 °C.

Interestingly, detailed ^{31}P{^{1}H} NMR analysis gave us further information on another source of the carbonyl ligands. The signal of **2** at δ = 48.7 was observed as an apparent triplet, whereas that of **3** at δ = 54.8 was observed as an apparent quintet. The splitting widths of these ^{31}P-signals were about halves of the corresponding J(CP) values observed in the ^{13}C{^{1}H} NMR. If the di- and tricarbonyl species were composed only of [Ru(^{13}CO)(^{12}CO)(PPh_3)$_3$] and [Ru(^{13}CO)$_2$(^{12}CO)(PPh_3)$_2$], respectively, a doublet and a triplet should be observed in the ^{31}P{^{1}H} NMR spectrum. The triplet and quintet with half splitting widths of the J(CP) values indicate the co-existence of some newly-formed ^{12}CO species. In other words, the apparent triplet is an overlap of the singlet of [Ru(^{12}CO)$_2$(PPh_3)$_3$] and the doublet of [Ru(^{13}CO)(^{12}CO)(PPh_3)$_3$], and the quintet is composed of the singlet of [Ru(^{12}CO)$_3$(PPh_3)$_2$], the doublet of [Ru(^{13}CO)(^{12}CO)$_2$(PPh_3)$_2$] and the triplet of [Ru(^{13}CO)$_2$(^{12}CO)(PPh_3)$_2$]. Hence, there must be another source of the ^{12}CO groups in the reaction mixture.

Even in the absence of the ester, complex **1** reacted with

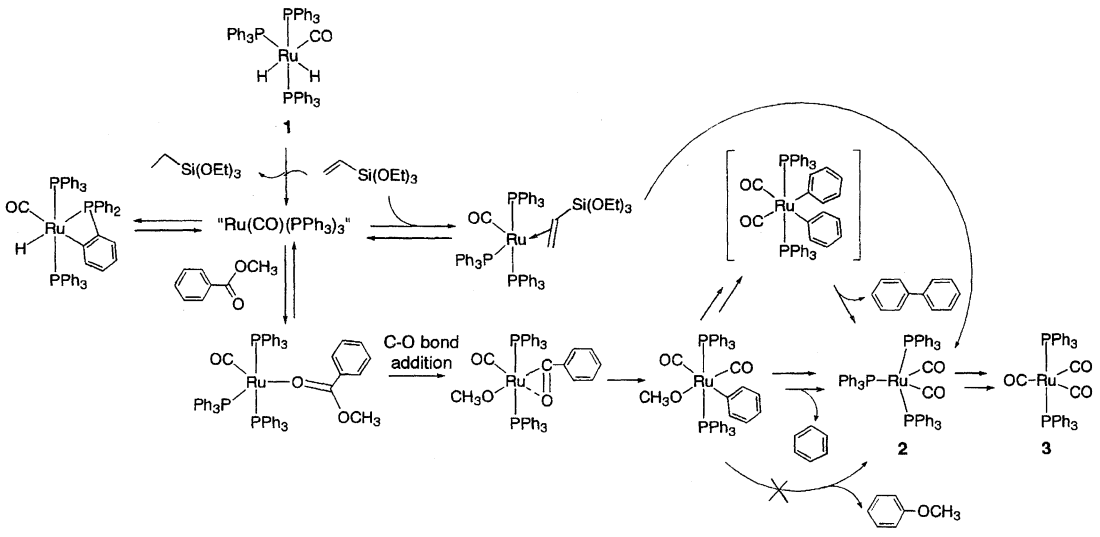

Scheme 2.

triethoxyvinylsilane in toluene-d_8 at 110 °C to afford the dicarbonyl species **2**. The tricarbonyl species **3** grew slowly with prolonged heating. These facts indicate that some of the second and the third carbonyl groups were derived also from the ethoxy group of triethoxyvinylsilane. Although Si–OCH_2CH_3 and OCH_2–CH_3 bonds are generally regarded very strong and stable, it is quite astonishing that these bonds of triethoxyvinylsilane are cleaved by the ruthenium-species. Previously, Komiya et al.[25] reported that $[RuH_2(PPh_3)_4]$ reacted with vinyloxy- and allyloxytrimethylsilanes to afford **1** and **3**, involving the cleavage of Si–O and OC–C bonds, whereas butoxytrimethylsilane did not react with $[RuH_2(PPh_3)_4]$ at 80 °C.

The ruthenium-promoted subtraction of the carbonyl group from the ester is illustrated as a sequence of the following steps that have been reported previously. The ester-coordinated species undergoes oxidative addition to yield an intermediate "$Ru(COPh)(OCH_3)(CO)(PPh_3)_2$". Similar acylruthenium(II) complexes $[Ru(\eta^2\text{-}COR)I(CO)(PPh_3)_2]$ were reported by Roper et al.[26] Then the carbonyl group of the benzoyl ligand is migrated to form a dicarbonyl(phenyl)ruthenium(II) complex "$RuPh(OCH_3)(CO)_2(PPh_3)_2$". The intermediary benzoylcarbonyl- and dicarbonyl(phenyl)ruthenium(II) complexes can be related to "$Rh(COMe)H(OAr)(PPh_3)_3$" and "$RhMeH(OAr)(CO)(PPh_3)_2$", respectively, which Yamamoto et al.[27] proposed as intermediates in the reaction course from $[RhH(PPh_3)_4]$ and aryl acetates to $[Rh(OAr)(CO)(PPh_3)_2]$ and methane.

It is possible to suppose the reductive elimination of anisole from the methoxo(phenyl)ruthenium(II) complex; nevertheless, detailed GC analyses of the reaction mixture detected no anisole, but benzene, biphenyl, and diethoxymethoxyvinylsilane together with small amounts of methyl *o*-[2-(triethoxysilyl)ethyl]benzoate and *o*-[2-(diethoxysilyl)ethyl]benzoate. Benzene is possibly derived by reductive elimination from a hydridophenylruthenium(II) species, which is formed by a ligand exchange reaction between the phenylruthenium(II) species and **1**. The detection of diethoxymethoxyvinylsilane and methyl *o*-[2-(diethoxysilyl)ethyl]benzoate suggests that active ruthenium species give rise to ligand exchange reactions among ethoxy, methoxy, and hydride groups. Biphenyl is probably formed by reductive elimination from a diphenylruthenium(II) species, which is derived by a disproportionation reaction between two molecules of the phenylruthenium(II) species. Yamamoto et al.[28] reported that $[Ni(cod)_2]$ reacted with phenyl propionate in the presence of PEt_3 to form $Ni(OPh)_2$, $[Ni(CO)_2(PEt_3)_2]$, and a 1 : 1 mixture of ethylene and ethane, but no phenetole, suggesting disproportionation reaction between two ethyl(phenoxo)nickel(II) species. Benzene and biphenyl are considered to be fates of "$RuPh(OCH_3)(CO)_2(PPh_3)_2$" when it is converted into "$Ru(CO)_2(PPh_3)_2$".

Competitive Reactions; C–H/Olefin Coupling and Formation of Di- and Tricarbonylruthenium(O) Species. The formation of methyl *o*-[2-(triethoxysilyl)ethyl]benzoate and its derivative is indicative of the coupling reaction between methyl benzoate and triethoxyvinylsilane. When the ester-coordinated "$Ru(CO)(PPh_3)_3L$" undergoes oxidative addition of the ortho C–H bond in place of the C–O bond of the ester, a hydrido(2-methoxycarbonylphenyl)ruthenium(II) intermediate "$Ru(C_6H_4COOCH_3)H(CO)(PPh_3)_2$" is produced instead of the other intermediate "$Ru(COPh)(OCH_3)(CO)(PPh_3)_2$" (Scheme 3). Successive insertion of triethoxyvinylsilane and reductive elimination of the coupling product regenerate the zerovalent species. This alternate route, however, is proved not to be predominant for methyl benzoate and *o*-toluate as shown above. Moreover, the di- and tricarbonyl complexes **2** and **3** produced via decarbonylation of the ester are much less reactive than **1**.[6] Therefore, only trace amounts of the C–H/olefin coupling products are detected in the reaction mixture.

Sonoda et al.[29] reported recently that *t*-butyl, phenyl, and 2, 2, 2-trifluoroethyl benzoates, methyl *p*-toluate, and methyl *p*-methoxybenzoate gave no C–H/olefin coupling product. In contrast to the low reactivity of these ordinary aromatic esters, surprisingly, the complex **1** was reported to catalyze the C–H/olefin coupling reaction in good yields when particular aromatic esters, such as ethyl thiophene-2-carboxylate, ethyl fluorobenzoates, and methyl trifluoromethylbenzoates are employed. Substituted propenoic acid esters also undergo C–H/olefin coupling at the β-position of the esters with a similar catalytic system.[7] We consider that these particular esters prevent the carbonyl subtraction and prefer to undergo the oxidative addition of the C–H bond when the intermediate "$Ru(CO)(PPh_3)_3L$" is formed. We have been exploring

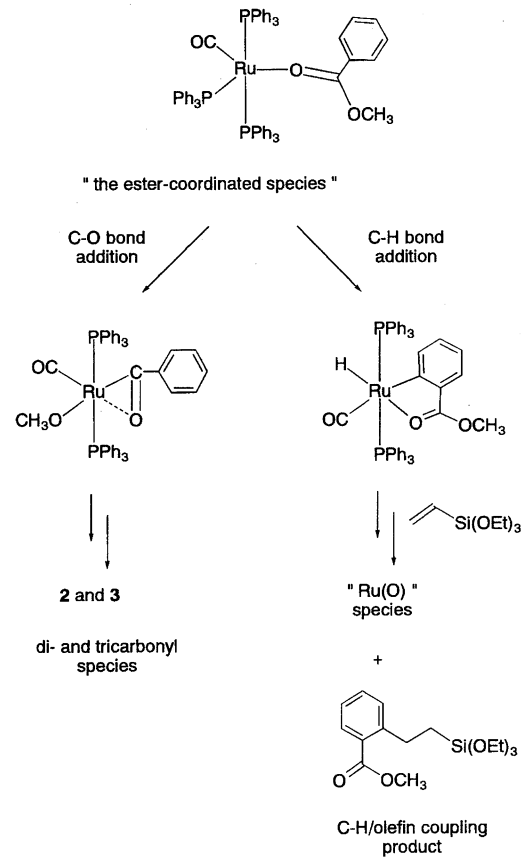

Scheme 3.

the definitive factors of the ester which determine whether it undergoes the C–H/olefin coupling or not. The detailed results shall be given in our forthcoming paper.

We have presumed the monocarbonylruthenium(O) species to be a common intermediate of the carbonyl subtraction and C–H/olefin coupling of the aromatic esters. On the other hand, Trost et al.[7] proposed a coordinatively unsaturated carbonyl-free "$Ru(PPh_3)_3L$" as an intermediate on the basis of the fact that the coupling reaction was strongly inhibited under a CO atmosphere. Under the CO atmosphere and in the presence of PPh_3, however, most ruthenium(O) species must have been converted into the catalytically less active tricarbonyl complex **3**.[30] The strong inhibition of the coupling can be interpreted as a result of the formation of **3** and, therefore, does not eliminate the monocarbonyl species from the possible intermediates of the reaction.

Experimental

General Comments. All experiments were performed in sealed tubes or standard Schlenk tubes under an inert atmosphere. All solvents were dried and distilled over appropriate drying agents and stored under nitrogen prior to use. $[RuH_2(CO)(PPh_3)_3]$ was prepared according to the literature.[31] Carbon-13 enriched $C_6H_5{}^{13}COOCH_3$ was purchased from Isotec Inc. Ohio, U.S.A. The ^{13}C content of its carbonyl group was more than 99%. All other reagents were purchased and used without further purification.

Infrared spectra were recorded on a JASCO A-100 spectrometer using KBr tablets. NMR spectra were obtained on a JEOL GX-400 spectrometer operating at 400 MHz for ^1H, 101 MHz for ^{13}C referenced to $SiMe_4$, and at 162 MHz for ^{31}P referenced to 85% H_3PO_4 in water. Single crystal X-ray structure analyses were performed on a Rigaku RASA-7 automatic structure analysis system, elemental analyses on a Yanaco MT-3 CHN Corder, and FAB- and GC-MS measurement on a JEOL JMS-DX303 mass spectrometer by the Center for Instrumental Analysis, Nagasaki University.

Synthesis of $[Ru(CO)_2(PPh_3)_3]$ (2). A suspension of **1** (82 mg, 0.09 mmol) in octane–toluene (8 : 1, 2.7 cm^3) containing methyl benzoate (31 mg, 0.22 mmol) and triethoxyvinylsilane (27 mg, 0.14 mmol) was heated in a sealed tube at 110 °C for 3 h. The resulting solution was cooled down slowly to about 5 °C to precipitate orange crystals, accompanied by a small amount of white solids. The seal was broken and the orange crystals were separated and collected under an inert atmosphere. Yield: 60 mg (80%). Found: C, 71.25; H, 4.80%. Calcd for $C_{56}H_{45}O_2P_3Ru$: C, 70.01; H, 4.90%. IR ν (C≡O) 1905 (vs), 1850 (w) cm^{-1}. $^{13}C\{^1H\}$ NMR (toluene-d_8) $\delta = 221.5$ (quartet, J (CP) = 13.7 Hz, RuCO). $^{31}P\{^1H\}$ NMR (toluene-d_8) $\delta = 48.7$.

Synthesis of $[Ru(CO)_3(PPh_3)_2]$ (3). A mesitylene solution (3 cm^3) of **1** (113 mg, 0.12 mmol), triethoxyvinylsilane (410 mg, 2.15 mmol), and methyl *o*-toluate (298 mg, 2.0 mmol) was heated at 160 °C for 4 h. The reaction mixture, then, was allowed to stand at room temperature for 10 h. Pale-yellow solids were precipitated and collected on a glass filter. The solids were washed with hexane several times to yield 40 mg (47%) of **3**. Found: C, 65.82; H, 4.48. IR ν (C≡O) 1895 (vs) cm^{-1}. $^{13}C\{^1H\}$ NMR (toluene-d_8) $\delta = 208.6$ (t, J (CP) = 17.6 Hz, RuCO). $^{31}P\{^1H\}$ NMR (toluene-d_8) $\delta = 54.8$.

Synthesis of $[Ru(\eta^2\text{-}O_2)(CO)_2(PPh_3)_2]$ (4). A mesitylene solution (3 cm^3) of **1** (118 mg, 0.13 mmol), triethoxyvinylsilane (597 mg, 3.14 mmol), and methyl *o*-toluate (68 mg, 0.45 mmol) was sealed in a glass tube and heated at 110 °C for 4 h. After being cooled down to room temperature, the reaction mixture was exposed to air for 12 h. Orange plates were precipitated and collected on a glass filter. The solids were washed with hexane several times to yield 33 mg (35%) of **4**. Found: C, 62.50; H, 4.53%. Calcd for $C_{38}H_{30}O_4P_2Ru$: C, 63.95; H, 4.25%. IR ν (C≡O) 2000 (vs), 1945 (vs) cm^{-1}. $^{13}C\{^1H\}$ NMR (CD_2Cl_2) $\delta = 199.4$ (t, J (CP) = 11.7 Hz, RuCO). $^{31}P\{^1H\}$ NMR (toluene-d_8) $\delta = 32.9$. FAB MS (matrix = CH_2Cl_2 and nitrobenzyl alcohol) m/z 713 [M − 1], 682 $[Ru(CO)_2(PPh_3)_2]$, 669 $[RuO(CO)(PPh_3)_2 - 1]$, 654[Ru(CO)-$(PPh_3)_2$], 641 $[RuO(PPh_3)_2 - 1]$, 625 $[Ru(PPh_3)_2 - 1]$, 392 [Ru-(CO)(PPh_3)], 379 $[RuO(PPh_3) - 1]$, 279 $[Ph_3P{=}O + 1]$, and 263 $[PPh_3 + 1]$.

NMR Studies: Stepwise Formation of 2 and 3. A suspension of **1** (20 mg, 0.02 mmol), methyl *o*-toluate (16 mg, 0.11 mmol) and triethoxyvinylsilane (83 mg, 0.44 mmol) in toluene-d_8 (0.75 cm^3) was sealed in an NMR tube. The suspension was heated at 110 °C for 3 h to turn into a pale-yellow solution. The $^{31}P\{^1H\}$ NMR spectrum of the reaction mixture showed seven apparent singlets at $\delta = -6.3$ (free PPh_3), 42.1, 45.3, 48.7 (**2**), 49.0, 54.8 (**3**), and 56.3, with relative intensities of 0.63, 0.03, 0.18, 1.00, 0.14, 0.09, and 0.20, respectively. When the reaction mixture was heated at 160 °C for a further 12 h, the $^{31}P\{^1H\}$ NMR spectrum of the reaction mixture turned into two singlets at $\delta = -6.3$ (free PPh_3) and 54.8 (**3**) with an intensity ratio of 1 : 2.

Reaction of 1 and Triethoxyvinylsilane without Ester. A toluene-d_8 (0.75 cm^3) suspension of **1** (40 mg, 0.04 mmol) and

Table 4. Crystal Data and Details of Measurements for Complexes **2** and **4**

	2	**4**
	Crystal data	
Formula	$C_{56}H_{45}O_2P_3Ru$	$C_{39}H_{30}O_4P_2Ru$
M	1059.80	713.67
Color and habit	Orange, quartz-like	Orange, plate
Crystal size/mm	0.30×0.10×0.35	0.20×0.15×0.50
Crystal system	Monoclinic	Triclinic
Lattice type	Primitive	Primitive
Space group	$P2_1/n$ (No.14)	$P\bar{1}$ (No.2)
a/Å	26.815(3)	9.936(1)
b/Å	12.809(3)	17.431(4)
c/Å	26.866(3)	9.876(3)
α/°		92.17(3)
β/°	95.677(10)	92.90(2)
γ/°		96.70(1)
V/Å^3	9182(2)	1695.0(6)
Z	8	2
D (calcd)/g cm^{-3}	1.366	1.398
$F(000)$	3888.00	728.00
μ(Mo $K\alpha$)/cm^{-1}	4.89	5.95
	Details of measurement and refinement	
Scan type	ω scan	ω–2θ scan
Scan width	$(0.68 + 0.30 \tan\theta)°$	$(1.63 + 0.30 \tan\theta)°$
2θ range	$4° < 2\theta < 50°$	$4° < 2\theta < 60°$
No. of reflections	16963	10406
No. of unique reflections	16584	9879
No. of observations ($I > 3\sigma(I)$)	6468	4001
No. of variables	1117	406
GOF	1.29	2.22
R, R_w	0.048, 0.035	0.066, 0.067

Table 5. Atomic Coordinates and Equivalent Temperature Factors for Non-Hydrogen Atoms of **2**

Atom	x	y	z	B(eq)	Atom	x	y	z	B(eq)
Ru(1)	0.11796(3)	0.05647(6)	−0.12186(3)	3.34(2)	C(184)	0.0039(5)	−0.308(1)	−0.1350(5)	12.5(6)
Ru(2)	0.11934(3)	−0.36861(6)	−0.60816(3)	2.74(2)	C(185)	0.0476(4)	−0.260(1)	−0.1467(4)	8.4(4)
P(11)	0.18300(8)	0.1308(2)	−0.16589(8)	3.08(6)	C(190)	0.1786(3)	−0.1914(7)	−0.0851(3)	3.1(2)
P(12)	0.06914(9)	0.2069(2)	−0.10921(9)	3.52(6)	C(191)	0.1704(3)	−0.2827(8)	−0.0611(4)	4.6(3)
P(13)	0.13032(9)	−0.1239(2)	−0.12712(8)	3.22(6)	C(192)	0.2097(4)	−0.3351(7)	−0.0335(4)	5.6(3)
P(21)	0.16540(9)	−0.3311(2)	−0.67930(8)	3.26(6)	C(193)	0.2570(4)	−0.2959(8)	−0.0313(3)	4.9(3)
P(22)	0.11133(8)	−0.2011(2)	−0.57450(8)	2.98(6)	C(194)	0.2660(3)	−0.2036(9)	−0.0559(3)	4.7(3)
P(23)	0.11908(9)	−0.5538(2)	−0.61150(8)	3.06(6)	C(195)	0.2267(4)	−0.1530(7)	−0.0816(3)	4.1(3)
O(11)	0.0254(3)	−0.0015(6)	−0.1940(3)	8.3(3)	C(210)	0.1530(3)	−0.4189(7)	−0.7332(3)	3.5(2)
O(12)	0.1601(4)	0.0278(7)	−0.0148(3)	10.6(3)	C(211)	0.1052(4)	−0.4563(8)	−0.7446(3)	4.3(3)
O(21)	0.0055(2)	−0.3580(6)	−0.6238(2)	6.0(2)	C(212)	0.0916(4)	−0.5112(8)	−0.7877(4)	5.7(3)
O(22)	0.1878(2)	−0.4035(5)	−0.5123(2)	5.7(2)	C(213)	0.1271(5)	−0.5331(10)	−0.8200(4)	7.8(4)
C(11)	0.0615(4)	0.0250(8)	−0.1676(4)	5.5(3)	C(214)	0.1744(5)	−0.499(1)	−0.8089(5)	7.8(4)
C(12)	0.1449(4)	0.0447(9)	−0.0564(4)	6.7(3)	C(215)	0.1880(3)	−0.4419(8)	−0.7666(3)	5.1(3)
C(21)	0.0498(3)	−0.3629(7)	−0.6206(3)	4.0(2)	C(220)	0.2342(3)	−0.3306(7)	−0.6676(3)	3.9(3)
C(22)	0.1631(3)	−0.3901(7)	−0.5507(3)	4.1(3)	C(221)	0.2653(4)	−0.2804(8)	−0.6980(3)	4.8(3)
C(110)	0.1715(3)	0.1484(7)	−0.2347(3)	3.4(2)	C(222)	0.3170(4)	−0.2789(8)	−0.6890(4)	5.6(3)
C(111)	0.2096(3)	0.1557(6)	−0.2655(3)	3.4(2)	C(223)	0.3390(3)	−0.3267(9)	−0.6468(4)	5.4(3)
C(112)	0.1994(4)	0.1714(7)	−0.3168(3)	4.4(3)	C(224)	0.3092(4)	−0.3792(8)	−0.6156(3)	4.9(3)
C(113)	0.1514(4)	0.1760(8)	−0.3377(3)	4.6(3)	C(225)	0.2578(3)	−0.3777(8)	−0.6261(3)	4.2(3)
C(114)	0.1130(4)	0.1707(8)	−0.3082(4)	5.4(3)	C(230)	0.1535(3)	−0.2056(7)	−0.7138(3)	3.3(2)
C(115)	0.1226(3)	0.1548(7)	−0.2564(3)	4.2(3)	C(231)	0.1196(4)	−0.2012(8)	−0.7561(4)	4.6(3)
C(120)	0.2451(3)	0.0659(7)	−0.1589(3)	3.2(2)	C(232)	0.1091(4)	−0.1077(9)	−0.7797(4)	5.6(3)
C(121)	0.2571(3)	−0.0128(7)	−0.1913(3)	3.2(2)	C(233)	0.1320(4)	−0.0178(8)	−0.7625(4)	5.5(3)
C(122)	0.3026(3)	−0.0637(7)	−0.1853(3)	3.9(3)	C(234)	0.1657(4)	−0.0221(7)	−0.7206(4)	5.2(3)
C(123)	0.3373(3)	−0.0379(8)	−0.1452(4)	4.4(3)	C(235)	0.1762(3)	−0.1159(8)	−0.6964(3)	4.4(3)
C(124)	0.3246(3)	0.0380(8)	−0.1121(3)	4.2(3)	C(240)	0.0585(3)	−0.1196(7)	−0.5989(3)	3.2(2)
C(125)	0.2800(3)	0.0899(7)	−0.1187(3)	3.7(2)	C(241)	0.0489(3)	−0.1112(8)	−0.6510(3)	4.2(3)
C(130)	0.2047(3)	0.2631(7)	−0.1457(3)	3.1(2)	C(242)	0.0113(4)	−0.0453(9)	−0.6712(3)	5.0(3)
C(131)	0.2239(4)	0.3344(7)	−0.1767(3)	4.5(3)	C(243)	−0.0158(4)	0.0130(9)	−0.6416(4)	6.1(3)
C(132)	0.2415(4)	0.4300(8)	−0.1605(4)	5.7(3)	C(244)	−0.0076(4)	0.0034(9)	−0.5908(4)	6.3(3)
C(133)	0.2405(4)	0.4549(8)	−0.1110(4)	5.5(3)	C(245)	0.0293(4)	−0.0624(8)	−0.5697(3)	5.1(3)
C(134)	0.2212(4)	0.3857(8)	−0.0790(3)	4.8(3)	C(250)	0.1636(3)	−0.1090(7)	−0.5751(3)	3.2(2)
C(135)	0.2037(3)	0.2888(7)	−0.0957(3)	3.7(2)	C(251)	0.1572(3)	−0.0038(8)	−0.5845(4)	4.5(3)
C(140)	0.0055(3)	0.1775(8)	−0.0938(3)	3.9(3)	C(252)	0.1970(4)	0.0626(8)	−0.5877(4)	5.3(3)
C(141)	−0.0060(4)	0.0794(8)	−0.0774(3)	4.7(3)	C(253)	0.2450(4)	0.0240(10)	−0.5796(4)	5.4(3)
C(142)	−0.0536(4)	0.0574(9)	−0.0633(4)	6.2(3)	C(254)	0.2527(4)	−0.0801(9)	−0.5685(3)	4.6(3)
C(143)	−0.0892(4)	0.135(1)	−0.0651(4)	6.3(4)	C(255)	0.2119(3)	−0.1451(7)	−0.5663(3)	4.0(3)
C(144)	−0.0793(4)	0.231(1)	−0.0809(5)	6.9(4)	C(260)	0.1015(3)	−0.2099(7)	−0.5075(3)	2.9(2)
C(145)	−0.0314(4)	0.2535(8)	−0.0949(4)	5.4(3)	C(261)	0.1338(3)	−0.1662(7)	−0.4700(3)	4.4(3)
C(150)	0.0575(3)	0.2869(7)	−0.1655(3)	3.8(3)	C(262)	0.1252(4)	−0.1798(8)	−0.4206(3)	5.3(3)
C(151)	0.0183(3)	0.2630(8)	−0.2022(4)	4.9(3)	C(263)	0.0850(4)	−0.2363(8)	−0.4084(3)	4.9(3)
C(152)	0.0127(4)	0.3120(9)	−0.2474(4)	5.7(3)	C(264)	0.0525(3)	−0.2787(7)	−0.4447(4)	4.3(3)
C(153)	0.0465(4)	0.3892(9)	−0.2572(4)	6.1(3)	C(265)	0.0612(3)	−0.2667(7)	−0.4944(3)	4.1(3)
C(154)	0.0848(4)	0.4167(8)	−0.2221(4)	5.6(3)	C(270)	0.0776(3)	−0.6308(7)	−0.6569(3)	3.4(2)
C(155)	0.0901(3)	0.3671(8)	−0.1765(3)	4.7(3)	C(271)	0.0291(4)	−0.6005(7)	−0.6678(4)	5.0(3)
C(160)	0.0845(3)	0.3060(8)	−0.0605(4)	4.0(3)	C(272)	−0.0058(4)	−0.6605(9)	−0.6985(5)	7.1(4)
C(161)	0.0713(4)	0.4099(8)	−0.0643(4)	5.6(3)	C(273)	0.0108(5)	−0.7521(9)	−0.7171(4)	6.8(4)
C(162)	0.0817(4)	0.4778(8)	−0.0251(4)	6.0(3)	C(274)	0.0585(5)	−0.7851(9)	−0.7065(5)	8.0(4)
C(163)	0.1061(4)	0.4448(10)	0.0199(4)	6.1(3)	C(275)	0.0920(4)	−0.7252(9)	−0.6768(4)	6.1(3)
C(164)	0.1182(4)	0.3417(9)	0.0250(4)	4.8(3)	C(280)	0.1815(3)	−0.6081(6)	−0.6167(3)	3.1(2)
C(165)	0.1081(3)	0.2728(7)	−0.0146(4)	4.3(3)	C(281)	0.1998(3)	−0.6198(8)	−0.6631(3)	4.3(3)
C(170)	0.1412(3)	−0.1802(7)	−0.1883(3)	3.2(2)	C(282)	0.2488(4)	−0.6470(8)	−0.6676(3)	4.9(3)
C(171)	0.1343(3)	−0.1217(8)	−0.2307(3)	4.0(2)	C(283)	0.2805(4)	−0.6665(8)	−0.6257(4)	5.6(3)
C(172)	0.1401(4)	−0.1637(9)	−0.2774(3)	5.2(3)	C(284)	0.2632(3)	−0.6574(8)	−0.5793(3)	4.5(3)
C(173)	0.1540(4)	−0.2656(9)	−0.2806(4)	5.3(3)	C(285)	0.2145(3)	−0.6290(7)	−0.5750(3)	3.6(2)
C(174)	0.1606(4)	−0.3270(8)	−0.2387(4)	4.8(3)	C(290)	0.1017(3)	−0.6149(7)	−0.5540(3)	3.3(2)
C(175)	0.1553(3)	−0.2830(8)	−0.1925(3)	4.2(3)	C(291)	0.1053(4)	−0.7221(8)	−0.5467(4)	5.1(3)
C(180)	0.0742(3)	−0.1956(7)	−0.1138(3)	3.6(2)	C(292)	0.0911(4)	−0.7700(8)	−0.5046(4)	5.8(3)
C(181)	0.0560(4)	−0.1831(8)	−0.0674(3)	4.8(3)	C(293)	0.0723(4)	−0.7113(10)	−0.4680(4)	5.3(3)
C(182)	0.0134(4)	−0.2359(10)	−0.0562(4)	6.5(4)	C(294)	0.0680(4)	−0.6055(9)	−0.4739(4)	5.5(3)
C(183)	−0.0123(5)	−0.295(1)	−0.0898(5)	10.5(5)	C(295)	0.0826(3)	−0.5592(7)	−0.5171(3)	3.9(3)

triethoxyvinylsilane (23 mg, 0.12 mmol) was sealed in an NMR tube and heated at 110 °C for 1 h. The $^{31}P\{^1H\}$ NMR spectrum of the reaction mixture showed six singlets at $\delta = -6.3$ (free PPh_3), 42.6, 45.3, 46.1, 48.7 (**2**), and 49.1 with relative intensity ratios of 0.35, 0.03, 0.08, 0.08, 1.00, and 0.09. In addition, small amounts of the starting **1** and an orthometallated hydridoruthenium(II) species were found in the mixture: The orthometallated complex $[Ru(C_6H_4PPh_2)H(CO)(PPh_3)_2]$[24] showed a doublet at $\delta = 50.3$ and a triplet at $\delta = -36.9$ with an A_2X pattern (^2J (PP) = 15Hz) in the $^{31}P\{^1H\}$ NMR spectrum and a double triplet at $\delta = -8.31$ (^2J (HP) = 83.9 Hz for d and 26.6 Hz for t) in the ^1H NMR one. After heating for a further 12 h at 110 °C, a singlet at $\delta = 54.8$ (**3**) appeared, whereas **1** disappeared.

Formation of 2 and 3 Using $C_6H_5{}^{13}COOCH_3$. A suspension of complex **1** (16 mg, 0.02 mmol), $C_6H_5{}^{13}COOCH_3$ (17 mg, 0.13 mmol) and triethoxyvinylsilane (25 mg, 0.13 mmol) in toluene-d_8 (0.6 cm^3) was sealed in an NMR tube. The suspension was heated at 110 °C for 3 h to turn into a pale-yellow solution. In the $^{13}C\{^1H\}$ NMR spectrum of the reaction mixture, signals of the carbonyls of **2** ($\delta = 221.5$, quartet, J (CP) = 13.7 Hz), the carbonyls of **3** ($\delta = 208.6$, t, J (CP) = 17.6 Hz), and the carbonyl of $C_6H_5{}^{13}COOCH_3$ were observed. No other signal was enhanced by the presence of $C_6H_5{}^{13}COOCH_3$. After the reaction mixture was heated at 160 °C for a further 3 h, the $^{13}C\{^1H\}$ NMR spectrum showed that the signal of **2** had disappeared and only that of **3** remained.

An apparent triplet of **2** and an apparent quintet of **3** were observed at $\delta = 48.7$ and 54.8, respectively, in the $^{31}P\{^1H\}$ NMR spectrum. The apparent coupling constants J (PC) based on the $^{31}P\{^1H\}$ NMR spectrum were 7.3 Hz for **2** and 8.0 Hz for **3**, which were approximately halves of the respective values based on the $^{13}C\{^1H\}$ NMR spectrum. The triplet was an overlap of a singlet of $[Ru(^{12}CO)_2(PPh_3)_3]$ and a doublet of $[Ru(^{13}CO)(^{12}CO)(PPh_3)_3]$. The quintet was an overlap of the signals of $[Ru(^{12}CO)_3(PPh_3)_2]$, $[Ru(^{13}CO)(^{12}CO)_2(PPh_3)_2]$, and $[Ru(^{13}CO)_2(^{12}CO)(PPh_3)_2]$.

GLC Analysis of the Reaction Mixture. A suspension of complex **1** (84 mg, 0.09 mmol), methyl benzoate (33 mg, 0.24 mmol) and triethoxyvinylsilane (39 mg, 0.20 mmol) in toluene (3 cm^3) was sealed in a glass tube. The suspension was heated at 110 °C for 3 h. The GLC analysis of the resulting mixture showed five new peaks. One of the five was attributed to benzene by means of coinjection with the authentic sample. The remaining four peaks were assigned as follows using MS(EI) analysis.

Diethoxymethoxyvinylsilane, m/z 177 [M+1]. Triethoxyethylsilane, m/z 193 [M+1]. Methyl *o*-[2-(diethoxysilyl)ethyl]benzoate, m/z 281 [M − 1]. The last peak consisted of two components: biphenyl (m/z 154 [M]) and methyl *o*-[2-(triethoxysilyl)ethyl] benzoate (m/z 325 [M − 1]).

Crystal Structure Analysis of 2 and 4. Crystal data and details of the measurement are summarized in Table 4. Good orange quartz-like crystals of **2** and orange plate crystals of **4** were precipitated from the respective reaction mixtures and selected for X-ray diffraction experiments. The crystal of **2** sealed in a glass capillary of 0.5 mm diameter and the crystal of **4** glued on a glass fiber were mounted on a Rigaku AFC7S diffractometer with graphite-monochromated Mo $K\alpha$ radiation. Cell constants were obtained from the least-squares refinement of the setting angles of 25 reflections in the range $10.09 \leq 2\theta \leq 22.54°$ for **2** and in the range $20.08 \leq 2\theta \leq 24.54°$ for **4**. During the data collection, the intensities of three representative reflections were measured after every 150 reflections; no variation was observed for **2** and the intensities decreased by −2.6% for **4**. A linear correction factor was applied to the data of **4** to account for this phenomenon. An empirical absorption correction based on azimuthal scans of several reflections was applied which resulted in transmission factors ranging from 0.93 to 1.00 for **2** and from 0.61 to 0.98 for **4**. The data were corrected for Lorentz and polarization effects.

Table 6. Atomic Coordinates and Equivalent Temperature Factors for Non-Hydrogen Atoms of **4**

Atom	x	y	z	B(eq)
Ru(1)	0.24239(8)	0.23457(4)	0.21662(8)	3.99(2)
P(1)	0.3461(2)	0.1355(1)	0.3255(2)	3.58(5)
P(2)	0.1380(3)	0.3409(1)	0.1340(3)	5.07(7)
O(1)	0.1146(8)	0.2260(4)	0.3787(8)	7.9(2)
O(2)	0.2253(8)	0.2892(4)	0.4046(8)	8.2(3)
O(3)	0.1294(10)	0.1220(5)	−0.0116(9)	9.4(3)
O(4)	0.4993(8)	0.2930(4)	0.0901(8)	7.7(2)
C(1)	0.175(1)	0.1658(6)	0.073(1)	7.1(3)
C(2)	0.3986(10)	0.2697(5)	0.137(1)	5.6(3)
C(10)	0.2432(8)	0.0416(4)	0.3201(8)	3.5(2)
C(11)	0.1057(10)	0.0379(5)	0.323(1)	6.7(3)
C(12)	0.025(1)	−0.0305(7)	0.319(2)	9.5(4)
C(13)	0.079(1)	−0.0967(6)	0.312(1)	6.9(3)
C(14)	0.216(1)	−0.0949(5)	0.311(1)	6.2(3)
C(15)	0.2984(9)	−0.0262(5)	0.3132(9)	4.7(2)
C(20)	0.3879(8)	0.1581(5)	0.5040(9)	3.8(2)
C(21)	0.3546(9)	0.1091(5)	0.6039(10)	4.7(2)
C(22)	0.393(1)	0.1289(7)	0.737(1)	6.1(3)
C(23)	0.470(1)	0.1936(8)	0.774(1)	7.2(4)
C(24)	0.509(1)	0.2445(7)	0.679(1)	7.3(4)
C(25)	0.467(1)	0.2278(6)	0.545(1)	6.1(3)
C(30)	0.5056(8)	0.1129(5)	0.2565(9)	3.8(2)
C(31)	0.6237(9)	0.1123(5)	0.3356(9)	5.1(3)
C(32)	0.7434(10)	0.0983(6)	0.279(1)	6.6(3)
C(33)	0.746(1)	0.0848(7)	0.144(1)	7.0(4)
C(34)	0.632(1)	0.0842(7)	0.065(1)	7.1(3)
C(35)	0.5133(10)	0.0999(6)	0.1191(10)	5.7(3)
C(40)	−0.0074(10)	0.3639(6)	0.225(1)	5.7(3)
C(41)	−0.019(1)	0.4361(6)	0.276(1)	7.3(4)
C(42)	−0.133(1)	0.4524(7)	0.348(1)	9.2(4)
C(43)	−0.232(1)	0.3946(8)	0.364(1)	9.0(4)
C(44)	−0.222(1)	0.3225(8)	0.308(2)	9.4(5)
C(45)	−0.110(1)	0.3073(6)	0.244(1)	7.7(4)
C(50)	0.082(1)	0.3325(5)	−0.047(1)	5.4(3)
C(51)	0.165(1)	0.3070(6)	−0.141(1)	6.1(3)
C(52)	0.133(1)	0.3036(7)	−0.279(1)	7.5(4)
C(53)	0.010(2)	0.3224(8)	−0.323(1)	8.7(5)
C(54)	−0.076(1)	0.3455(8)	−0.235(2)	8.7(5)
C(55)	−0.046(1)	0.3515(7)	−0.093(1)	7.8(4)
C(60)	0.2552(10)	0.4302(5)	0.146(1)	5.6(3)
C(61)	0.339(1)	0.4466(6)	0.260(1)	8.4(4)
C(62)	0.434(2)	0.5120(8)	0.271(2)	10.6(6)
C(63)	0.445(2)	0.5598(9)	0.168(2)	11.6(7)
C(64)	0.359(2)	0.5470(7)	0.055(2)	10.0(5)
C(65)	0.261(1)	0.4807(6)	0.041(1)	7.1(3)

The structure of **2** was solved by Patterson methods[32] and expanded using Fourier techniques.[33] All non-hydrogen atoms were refined anisotropically. Hydrogen atoms were included but not refined. The final cycle of full-matrix least-squares refinement was based on 6468 observed reflections $\{I > 3\sigma(I)\}$ and 1117 variable parameters; the function minimized was $\Sigma w(|F_o| - |F_c|)^2$, where $w^{-1} = \sigma^2(F_o) + (0.002F_o)^2$. Final R and R_w values were 0.048 and 0.035, respectively $\{R = \Sigma||F_o| - |F_c||/\Sigma|F_o|$, $R_w = [\Sigma w(|F_o| - |F_c|)^2 / \Sigma wF_o{}^2]^{1/2}\}$.

The structure of **4** was solved by heavy-atom Patterson methods[34] and expanded using Fourier techniques.[33] All non-hydrogen atoms were refined anisotropically. Hydrogen atoms were included but not refined. The final cycle of full-matrix least-squares refinement was based on 4001 observed reflections $\{I > 3\sigma(I)\}$ and 406 variable parameters; the function minimized was $\Sigma w(|F_o| - |F_c|)^2$, where $w^{-1} = \sigma^2(F_o) + (0.01F_o)^2$. Final R and R_w values were 0.066 and 0.067, respectively, $\{R = \Sigma||F_o| - |F_c||/\Sigma|F_o|$, $R_w = [\Sigma w(|F_o| - |F_c|)^2/\Sigma wF_o^2]^{1/2}\}$.

Neutral atom scattering factors, corrected for anomalous dispersion, were taken from the literature.[35] All calculations were performed on a Rigaku RASA-7 automatic structure analysis system using the teXsan crystallographic software package.[36]

The final atomic coordinates and equivalent isotropic temperature factors for non-hydrogen atoms are listed in Tables 5 and 6. Tables of the anisotropic temperature factors for non-hydrogen atoms, the atomic coordinates and the temperature factors for hydrogen atoms, the complete lists of bond distances and angles, as well as the observed and calculated structure factors are deposited as Document No. 70016 at the Office of the Editor of Bull. Chem. Soc. Jpn.

The present work was partially supported by a Grant-in-Aid for Scientific Research on Priority Area of Reactive Organometallics No. 7216257 from the Ministry of Education, Science, Sports and Culture.

References

1) a) T. Mitsudo, Y. Nakagawa, K. Watanabe, Y. Hori, H. Misawa, H. Watanabe, and Y. Watanabe, *J. Org. Chem.*, **50**, 565 (1985); b) T. Mitsudo, Y. Hori, and Y. Watanabe, *J. Organomet. Chem.*, **334**, 157 (1987).

2) T. Naota, H. Taki, M. Mizuno, and S.-I. Murahashi, *J. Am. Chem. Soc.*, **111**, 5954 (1989).

3) a) B. M. Trost and R. J. Kulawiec, *J. Am. Chem. Soc.*, **114**, 5579 (1992); b) B. M. Trost and A. Indolese, *J. Am. Chem. Soc.*, **115**, 4361 (1993).

4) T. Rappert and A. Yamamoto, *Organometallics*, **13**, 4984 (1994), and literatures cited therein.

5) R. H. Grubbs, S. J. Miller, and G. C. Fu, *Acc. Chem. Res.*, **28**, 446 (1995), and literatures cited therein.

6) a) S. Murai, F. Kakiuchi, S. Sekine, Y. Tanaka, A. Kamatani, M. Sonoda, and N. Chatani, *Nature*, **366**, 529 (1993); b) F. Kakiuchi, S. Sekine, Y. Tanaka, A. Kamatani, M. Sonoda, N. Chatani, and S. Murai, *Bull. Chem. Soc. Jpn.*, **68**, 62 (1995).

7) B. M. Trost, K. Imi, and I. W. Davies, *J. Am. Chem. Soc.*, **117**, 5371 (1995).

8) a) F. Kakiuchi, Y. Tanaka, T. Sato, N. Chatani, and S. Murai, *Chem. Lett.*, **1995**, 679; b) F. Kakiuchi, Y. Yamamoto, N. Chatani, and S. Murai, *Chem. Lett.*, **1995**, 681; c) F. Kakiuchi, M. Yamauchi, N. Chatani, and S. Murai, *Chem. Lett.*, **1996**, 111.

9) N. Chatani, T. Fukuyama, F. Kakiuchi, and S. Murai, *J. Am. Chem. Soc.*, **118**, 493 (1996).

10) a) Y.-G. Lim, Y. H. Kim, and J.-B. Kang, *J. Chem. Soc., Chem. Commun.*, **1994**, 2267; b) Y.-G. Lim, J.-B. Kang, and Y. H. Kim, *J. Chem. Soc., Chem. Commun.*, **1996**, 585.

11) a) K. Hiraki, N. Ochi, T. Kitamura, Y. Sasada, and S. Shinoda, *Bull. Chem. Soc. Jpn.*, **55**, 2356 (1982); b) K. Hiraki, N. Ochi, Y. Sasada, H. Hayashida, Y. Fuchita, and S. Yamanaka, *J. Chem. Soc., Dalton Trans.*, **1985**, 873.

12) K. Hiraki, Y. Fuchita, H. Kawabata, K. Iwamoto, T. Yoshimura, and H. Kawano, *Bull. Chem. Soc. Jpn.*, **65**, 3027 (1992).

13) K. Hiraki, T. Matsunaga, and H. Kawano, *Organometallics*, **13**, 1878 (1994).

14) B. E. Cavit, K. R. Grundy, and W. R. Roper, *J. Chem. Soc., Chem. Commun.*, **1972**, 60.

15) R. S. Berry, *J. Chem. Phys.*, **32**, 933 (1960).

16) A. G. Orpen, L. Brammer, F. H. Allen, O. Kennard, D. G. Watson, and R. Taylor, *J. Chem. Soc., Dalton Trans.*, **1989**, S1.

17) a) M. Ogasawara, S. A. Macgregor, W. E. Streib, K. Folting, O. Eisenstein, and K. G. Caulton, *J. Am. Chem. Soc.*, **117**, 8869 (1995); b) M. Ogasawara, S. A. Macgregor, W. E. Streib, K. Folting, O. Eisenstein, and K. G. Caulton, *J. Am. Chem. Soc.*, **118**, 10189 (1996).

18) a) M. Ogasawara, F. Maseras, N. Gallego-Planas, W. E. Streib, O. Eisenstein, and K. G. Caulton, *Inorg. Chem.*, **35**, 7468 (1996); b) C. Li, M. Ogasawara, S. P. Nolan, and K. G. Caulton, *Organometallics*, **15**, 4900 (1996).

19) T. R. Gaffney and J. A. Ibers, *Inorg. Chem.*, **21**, 2851 (1982).

20) J. P. Collman and W. R. Roper, *J. Am. Chem. Soc.*, **87**, 4008 (1965).

21) M. Helliwell, J. D. Vessey, and R. J. Mawby, *J. Chem. Soc., Dalton Trans.*, **1994**, 1193.

22) J. A. McGinnety, N. C. Payne, and J. A. Ibers, *J. Am. Chem. Soc.*, **91**, 6301 (1969).

23) M. J. Bennett and P. B. Donaldson, *Inorg. Chem.*, **16**, 1581 (1977).

24) a) W. R. Roper and L. J. Wright, *J. Organomet. Chem.*, **234**, C5 (1982); b) G. R. Clark, C. E. L. Headford, K. Marsden, and W. R. Roper, *J. Organomet. Chem.*, **231**, 335 (1982).

25) S. Komiya, R. S. Srivastava, A. Yamamoto, and T. Yamamoto, *Organometallics*, **4**, 1504 (1985).

26) W. R. Roper, G. E. Taylor, J. M. Waters, and L. J. Wright, *J. Organomet. Chem.*, **182**, C46 (1979).

27) T. Yamamoto, S. Miyashita, Y. Naito, S. Komiya, T. Ito, and A. Yamamoto, *Organometallics*, **1**, 808 (1982).

28) T. Yamamoto, J. Ishizu, T. Kohara, S. Komiya, and A. Yamamoto, *J. Am. Chem. Soc.*, **102**, 3758 (1980).

29) M. Sonoda, F. Kakiuchi, A. Kamatani, N. Chatani, and S. Murai, *Chem. Lett.*, **1996**, 109.

30) a) J. Powell and B. L. Shaw, *J. Chem. Soc. A*, **1968**, 159; b) R. B. King and P. N. Kapoor, *Inorg. Chem.*, **11**, 336 (1972); c) S. Cenini, A. Mantovani, A. Fusi, and M. Keubler, *Gazz. Chim. Ital.*, **105**, 255 (1975).

31) N. Ahmad, J. J. Levison, S. D. Robinson, and M. F. Uttley, *Inorg. Synth.*, **15**, 48 (1974).

32) P. T. Beurskens, G. Admiraal, G. Beurskens, W. P. Bosman, S. Garcia-Granda, R. O. Gould, J. M. M. Smits, and C. Smykalla, "PATTY, The DIRDIF Program System, Technical Report of the Crystallography Laboratory," University of Nijmegen, The Netherlands (1992).

33) P. T. Beurskens, G. Admiraal, G. Beurskens, W. P. Bosman, S. Garcia-Granda, R. O. Gould, J. M. M. Smits, and C. Smykalla, "DIRDIF92, The DIRDIF Program System, Technical Report of the Crystallography Laboratory," University of Nijmegen, The Netherlands (1992).

34) Fan Hai-Fu, "SAPI 91, Structure Analysis Programs with Intelligent Control," Rigaku Corporation, Tokyo, Japan (1991).

35) "International Tables for X-Ray Crystallography," Kynoch Press, Birmingham, England (1974), Vol. IV.

36) "teXsan, Crystal Structure Analysis Package," Molecular Structure Corporation, (1985 and 1992).